

Parameter Optimization and Microstructure Evolution of In-Situ TiC Particle Reinforced Ni-based Composite Coating by Laser Cladding

Ma Shibang^{1*}, Du Zhihao¹, Xia Zhenwei², Xu Yang², Li Chao¹, and Shi Houjie³

¹School of Mechatronic Engineering, Nanyang Normal University, Nanyang 473061, China

²College of Engineering, China Agricultural University, Beijing 100083, China

³Department of Biological Systems Engineering, Washington State University, Pullman, 98101, United States

Received 19 December 2017; Accepted 5 April 2018

Abstract

Laser cladding is one of the most effective ways of improving the abrasion resistance and corrosion resistance of surfaces and is thus widely used to reinforce steel surfaces. This study aimed to investigate the effects of laser parameters on the properties of the composite layer and the reinforcement of Ni-based composite powder on a steel surface by laser cladding. The laser cladding of Ni-based Ni60A+x%(SiC+Ti) composite powder on 45 steel surface to form TiC particle reinforced coating was evaluated by the preplaced-powder method. The effects of laser power and scanning speed on mechanical property and hardness were assessed. Microstructure, phase composition, and energy spectrum were comprehensively analyzed by scanning electron microscopy, X-ray diffraction, and energy-dispersive spectrometry, respectively. Results reveal that the use of composite powder to form a reinforced coating on the 45 steel is feasible. At 24% SiC+Ti content, a cladding layer with a compact and homogeneous microstructure is obtained at 800 W laser power and 125 mm/min scanning speed. Numerous dispersedly distributed TiC particles exist at the cladding layer, and the size and number of TiC particles gradually increase with increase SiC+Ti content. The findings in this study provide insight into the application and promotion of laser cladding on 45 steel materials.

Keywords: Laser cladding, In-situ reaction, Parameters optimization, Microstructure evolution, Reinforced TiC particles

1. Introduction

Wear, corrosion, and fatigue damage are the main causes of steel failure, especially under humid environment and high friction conditions [1]. The wear, corrosion, and fatigue damage of steel parts mostly initiate on the surface. To prolong the service time of parts, various surface treatment technologies have been proposed for improving the performance of the matrix. Laser cladding is an advanced surface modification technology, in which high-energy laser beam is used to melt the surface of the substrate material and form a coating with a special function. This approach can fabricate high-performance surfaces with low-cost materials while reducing the energy consumption and cost [2,3]. The material and process parameters are the main factors determining the performance of the cladding layer. At present, powder materials, such as metal, ceramic, and composite powders, are the most widely used cladding materials. Given its good wettability, corrosion resistance, wear resistance, self-lubrication effect, and moderate price, Ni-based self-melting alloy powder has been widely studied and applied [4,5]. Sound metallurgical bonding has been achieved by cladding Ni alloy on 45 steel substrates [6]. High-temperature abrasion resistance and corrosion resistance can be improved by adding a ceramic phase to the cladding material [7-9]. In view of the significant differences

in thermal parameters and the poor compatibility of the ceramic phase and the metal matrix, cracks occur easily, and ceramic particles may be peeled from the matrix [10,11]. However, the in-situ reinforced phase is well compatible with the metal matrix, and the dispersed distribution of the reinforced phase can increase the toughness of the coating [12]. Laser cladding in-situ self-reinforced coating has been studied extensively [13-16]. The selected reinforced element and process parameters in laser cladding greatly affect the performance of the cladding layer, the cost, and further applications. Therefore, the appropriate reinforced elements must be selected, and the laser cladding process parameters must be optimized.

Therefore, this study aimed to use the preset of powder and orthogonal method to the process and structural properties of in-situ composite coating on steel surface by laser cladding. This main objective is to determine the appropriate in-situ reinforced elements and the best process parameters. The findings of this study can serve as a reference for the process optimization and application of in-situ composite coating by laser cladding.

2. State of the art

Many studies have investigated the laser cladding in-situ formed process. The carbides of Ti [17], W [18], Si [19], Cr and Zr [20], boride [21] and some oxide [22] are the main in-situ reinforced phases. Lo K.H. et al. [23] explored the dispersion of fine WC powder on AISI 316 stainless steel to improve the cavitation erosion resistance and the abrasion

*E-mail address: mshibang@126.com

ISSN: 1791-2377 © 2018 Eastern Macedonia and Thrace Institute of Technology. All rights reserved.

doi:10.25103/jestr.112.13

resistance by using a laser surfacing technique. The cavitation erosion resistance and abrasion resistance of the surface alloy layer of the specimens were significantly improved, and the cavitation resistance of laser composite surfaced AISI 316 stainless was enhanced by up to 30 times that of the as-received AISI 316 stainless steel. However, the brittleness of the coating was significant. S.K. Ghosh et al. [24] examined the crack density and wear resistance of the SiC particulate reinforced Al-based metal matrix composite. Although the abrasion resistance of the alloy composite material was significantly improved, the SiC ceramic phase easily produced a brittle phase at high temperature, which was unfavorable to the wear resistance and the corrosion resistance. Bandar A. et al. [25] investigated the effects of the applied laser energy density on the densification, microstructure, and mechanical properties of the selective laser melting processed parts, and they elucidated the mechanisms underlying the formation of TiC particles. The TiC reinforced phase exhibited good toughness, good lubricity, thermal and chemical stability, good wear resistance, and so on. It significantly improved the hardness, compressive strength, and corrosion resistance of the composite coating. However, this study did not consider the effect of different power parameters on the coating performance. Zhang L. et al. [26] investigated the influence of laser power on the microstructure and properties of Co-based amorphous composite coatings produced by laser cladding on a 45 medium steel substrate. Their results demonstrated that as the laser power was increased, the average hardness of the cladding layer decreased, whereas the abrasion resistance increased. However, they did not evaluate the effect of laser scanning speed. Ali E. et al. [27] found that the laser cladding parameters greatly influenced the TiC morphology. Chinmaya K. S. et al. [28] attempted to produce TiC reinforced composite coating on AISI 304 stainless steel through a preplaced laser surface engineering process by using a pulse laser to increase the hardness of the steel substrate. Their results showed that the laser peak power significantly affected the micro-hardness of the cladding layer. However, they also did not study the effect of laser scanning speed. Zeng CH. et al. [29] examined the relationship between the gas hole and laser power of laser-cladding deposited Ni-based coatings. Their results indicated that the porosity damage in the coating followed a Weibull distribution rather than a normal or lognormal distribution. However, they did not explain the relationship between porosity damage and laser scanning speed. Guo Y. Q. et al. [30] prepared an in-situ formed TiC particle reinforced Ni-base composite coating on H13 steel substrate by laser cladding and examined the micro-hardness and wear resistance of the laser cladding layer. This method had a high process requirements, resulting in its poor practical application. Li S.N. et al. [31] discussed the feasibility of using Ti and SiC powders to fabricate a TiC composite coating via in-situ laser cladding. However, the effects of specific process parameters on the properties of the composite coating were not comprehensively analyzed.

Although the aforementioned works have mainly focused on the effects of laser power and scanning speed, their influence on the mechanical properties of the coating has yet to be clarified. Studies on the use of SiC and Ti powders as raw materials in fabricating TiC particles via in-situ reactions are also lacking. In the present work, we attempted to develop an in-situ TiC dispersed 45 steel-based metal matrix composite layer onto the 45 steel surface to improve its properties. The microstructure, phase, and

composition of the surface composite layer (processed under optimum conditions) were comprehensively analyzed to understand the effect of the laser process on the characteristics of the surface layer. The optimized process parameters of the laser cladding were determined.

The remainder of this study is organized as follows. Section 3 describes the experimental materials and methods. Section 4 analyzes the effects of power and scanning speed on the macroscopic quality and hardness as well as, the microstructure. The conclusions are summarized in Section 5.

3. Experimental material and method

In this work, 45 steel was chosen as the substrate material, Ni60A was used as the bonding phase, and SiC and Ti powders were used as the raw materials to generate a TiC reinforced phase. The in-situ reaction equation of TiC particles with SiC and Ti as the raw materials is expressed as follows:



The 45 steel samples with gauge dimensions of 135 mm × 110 mm × 10mm were prepared by electro-discharge machining. The surfaces of these samples were sand-blasted prior to laser processing to remove the oxide scale and then ultrasonically cleaned in alcohol to eliminate the dirt and the oil. Ni-based Ni60A+(SiC+Ti) composite powder with SiC:Ti=1:1 (at.%) was used the cladding material. The weight contents of SiC+Ti were set to 12%, 24%, 36%, 48%, and 60%. The chemical composition of the Ni60A alloy powder is presented in Table1. The composite powder was completely mixed and ground to guarantee homogeneity. 5% polyvinyl alcohol solution was used as the adhesive to bond the preplaced powder. After the preplaced powder was naturally dried, the TruDiod4006 semiconductor laser processing system was used to conduct the cladding experiment (Fig. 1).

To preplace the powder and ensure the thickness of the powder layer, a groove with gauge dimensions of 40 mm × 5 mm × 1 mm was milled, and the preplaced powder layer was set to 1 mm. The preset of the cladding powder is shown in Fig. 2. Laser energy density P_w ($W \cdot s \cdot mm^{-2}$) was introduced to examine the influence of laser power P and scanning speed ν on the properties of the cladding layer.

The equations describing the relationships among the laser power P , the laser facula area S , and the scan speed ν are as follows:

$$P_w = Pt / S \quad (2)$$

$$t = 60D / \nu \quad (3)$$

$$S = \pi(D/2)^2 \quad (4)$$

The equation for the activation energy P_w can be transformed from Eqs. (2)-(4) as follows:

$$P_w = 1.27 \cdot 60P / (D \cdot \nu) \quad (5)$$

where D (mm) is the diameter of laser facula, $t(s)$ is the scanning time of the unit area, S is the area of the laser

facula, and π is a constant (3.14). Orthogonal method was used, and the parameters of the laser cladding are shown in Table 2. The diameter of the laser facula was 2.5 mm, and the fixed defocus was 30 mm. Ni60A+24%(SiC+Ti) composite powder was used to investigate the laser cladding process. The post-laser cladding microstructure was characterized by scanning electron microscopy (SEM) with a Leica-S440i-SEM machine. Elemental analysis was conducted by energy disperse spectroscopy (EDS). Phase qualitative analysis was performed by X-ray diffraction (XRD) with a D/MAX2500-XRD machine. The hardness of the cladding layer was measured using a HT320 Rockwell Hardness Tester.

Table 1. Chemical composition of the Ni60A alloy powder

Element	Cr	B	Si	C	Fe	Ni
Mass fraction/%	17.0	3.5	4.0	1.0	<5.0	Bal

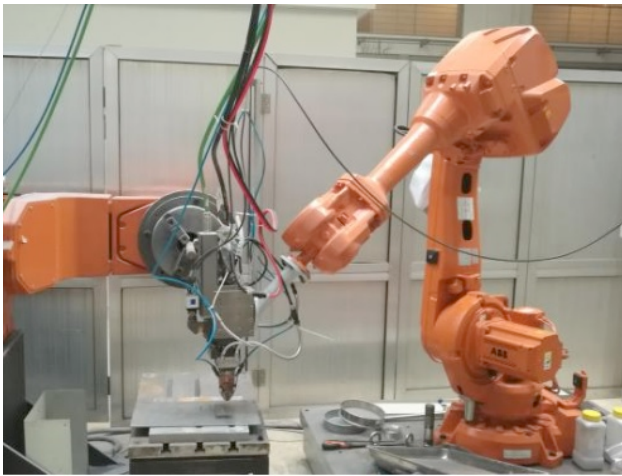


Fig. 1. Laser cladding system



Fig. 2. Preset of the cladding powder

Table 2. Parameters of the laser cladding of orthogonal test selection

Coating No.	P(W)	V(mm/min)	Pw(W·s·mm ⁻²)
A1	400	100	121.9
A2	600	100	182.9
A3	800	100	243.8
A4	1000	100	304.8
A5	1200	100	365.8
B1	400	125	97.5
B2	600	125	146.3
B3	800	125	195.1
B4	1000	125	243.8

B5	1200	125	292.6
C1	400	150	81.3
C2	600	150	121.9
C3	800	150	162.6
C4	1000	150	203.2
C5	1200	150	243.8

4 Results and discussion

4.1 Macroscopic morphology of the cladding layer

4.1.1 Influence of laser power on the macrostructure

Fig. 3 shows the macrostructures of the cladding layer at different laser power values and a scanning speed of 125 mm/min. The width of the coating gradually increased as the laser power was increased. At a low laser power of 400 W, the cladding layer was narrow and discontinuous. The width slightly increased at the laser power of 600 W. The cladding layer achieved an appropriate width and a smooth surface when the laser power was 800 and 1000 W. As the power reached 1200 W, the groove became filled with the cladding layer, and the surface became over-burned. Thus, the optimal laser power was determined to be between 800 and 1000 W.



Fig. 3. Macro morphology of the cladding layer at different laser power values

4.1.2 Influence of scanning speed on the macrostructure

Fig. 4 shows the macrostructures of the cladding layer at three different scanning speeds at the power of 800 W. The width varied slightly, and the surface was smooth, indicating that the selected range of scanning speed was appropriate, and that the effects of the different scanning speeds on the macrostructure were not evident.

4.2 Hardness of the cladding layer

4.2.1 Influence of laser power on hardness

Fig. 5 shows the influence of laser power on the hardness of the cladding layer (Ni60A+24% (SiC+Ti)). At a constant scanning speed, the hardness increased as the laser power increased. It reached the maximum value at the laser power of 800 W and then declined as the power continued to increase. The maximum hardness values were 70.02, 68.2,

and 70.1 HRA at the scanning speeds of 100, 125, and 150 mm/min, respectively.

Results indicated that laser power exerted an obvious effect on the hardness. At 400 W, the laser power was too low to completely melt the composite powder to form TiC particles; thus, fine dendrites cannot be formed, resulting in the low hardness. At 800 W, carbide and fine dendrites appeared, and the hardness increased as the laser power increased. Thus, the hardness reached the maximum value due to the optimal microstructure. Beyond that, the power was excessively high, such that the composite powder melted excessively, and the dendrite microstructures coarsened. Thus, the matrix element diluted to the cladding layer, leading to the hardness reduction.

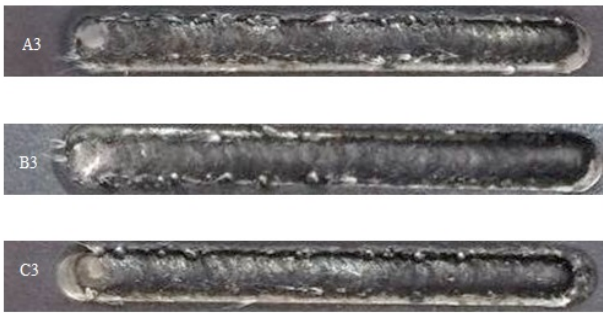


Fig. 4. Macro morphology of the cladding layer at different scanning speeds

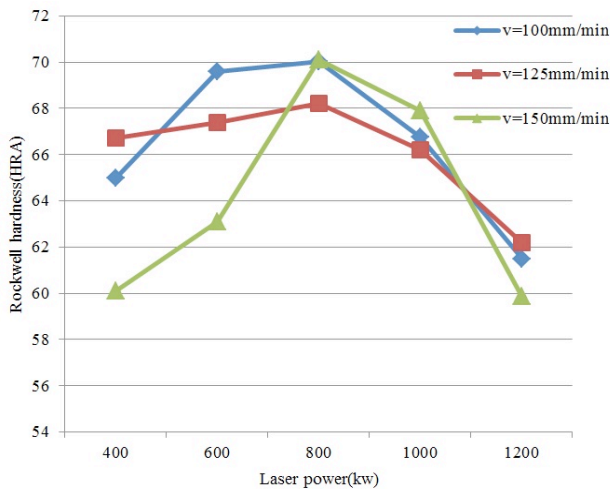


Fig. 5. Effect of laser power on the hardness of the cladding layer

4.2.2 Influence of scanning speed on hardness

Fig. 6 shows the influence of scanning speed on the hardness of the cladding layer (Ni60A+24% (SiC+Ti)). As shown, the effect was insignificant. When the laser power was 600 W, the maximum hardness was attained at the speed of 100 mm/min. When the laser power was 400 and 1200 W, the maximum hardness was achieved at the speed of 125 mm/min. The maximum hardness was reached at the speed of 125 mm/min at the laser power of 800 and 1000 W. The absorbed energy was negatively correlated with the scanning speed. The melting degree of the composite powder positively influenced the absorbed energy. In theory, the hardness of the cladding layer should initially increase and subsequently decrease; however, this phenomenon did not occur because of the small number of variable speeds, the low gradient of the speed variation, and the small number of samples. The speed of 125 mm/min can be considered the optimal scanning speed.

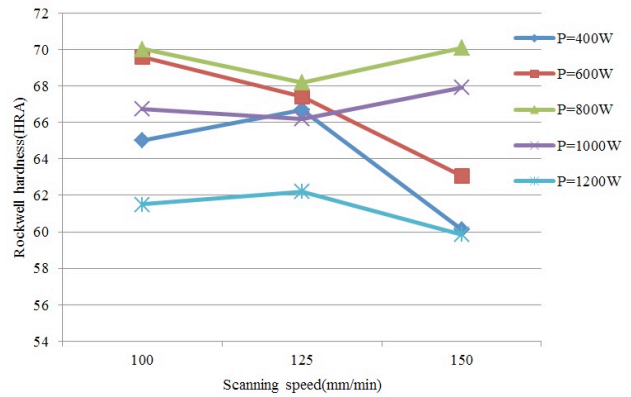


Fig. 6. Effect of scanning speed on the hardness of the cladding layer

4.3 Microstructure

4.3.1 Phase analysis of the cladding layer

The mechanical property depends on the microstructure. Fig. 7 shows the XRD pattern of the coating formed at the laser power of 800 W and the scanning speed of 125mm/min. The main phases were the solid solution of (Fe, Ni), the intermetallic $Cr_{1.36}Fe_{0.52}$, the eutectic compound of $Ni_{16}Cr_6Si_7$, and the carbide of TiC. These results suggested that TiC particles can be formed in situ by using SiC and Ti powder as the raw materials.

The diffraction peaks of (Fe, Ni) and $Cr_{1.36}Fe_{0.52}$ were high. In the laser cladding process, the composite powder and the matrix surface were melted, and Fe was diluted to the cladding layer. The electronegativity and atomic radius of Ni, Fe, and Cr were similar. The face-centered cubic lattice structure consisted of γ -Fe and Ni. Thus, the γ -(Ni, Fe) solid solution and the intermetallic $Cr_{1.36}Fe_{0.52}$ were easily formed under the melting condition. Phase retrieval revealed that SiC did not exist in the coating, implying that it was completely decomposed at high temperatures. The affinity with C of Ti was better than that of Cr, and the Ti-to-C atom proportion was 1:1. Thus, TiC was formed, and no Cr-C occurred. The combination reaction of Cr with Si and Fe formed $Cr_{1.36}Fe_{0.52}$ and $Ni_{16}Cr_6Si_7$. The laser cladding process is a non-equilibrium process of rapid solidification, and metastable and intermediate phases are formed. These phases are sensitive to the solidification condition and prone to the lattice distortion. Thus, a number of diffraction peaks that cannot be matched was present.

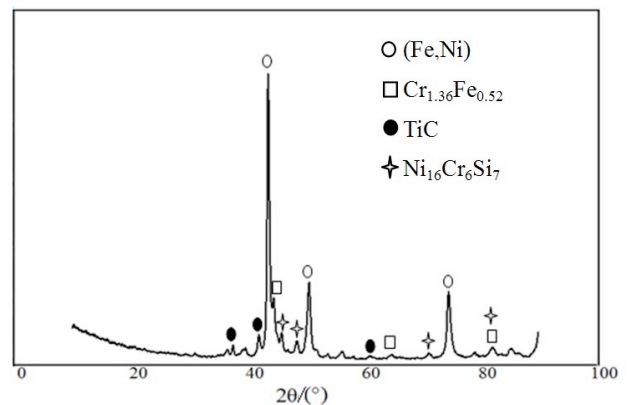


Fig. 7. XRD spectrum of the Ni60A+24%(SiC+Ti) composite coating

4.3.2 Energy spectrum analysis of the cladding layer

The chemical composition of the microstructure can be

confirmed by energy spectrum analysis. As shown in Fig. 8, the microstructure of the cladding layer displayed three different phases. The dark gray phase was the dendritic structure, the white phase was the eutectic microstructure, and the other one represented the white particles that were homogeneously distributed. EDS was conducted on the three different phases, and the measured position is shown in Fig. 8. The compositions of the different points are provided in Table 3. Fe was enriched at the cladding layer, demonstrating that an atomic diffusion occurred between the composite coating and the matrix. Such diffusion was beneficial for improving the bonding strength. Considerable amounts of Fe, Ni, and Si existed at the matrix, suggesting that the main dendritic phase was the (Ni,Fe) solution. The main phases of the eutectic structure were $Cr_{1.36}Fe_{0.52}$ and $Ni_{16}Cr_6Si_7$. The white phase of TiC can be determined by the contents of Ti and C. The size of the TiC particles was smaller than the diameter of the electron beam of the energy spectrometer, causing the collection range of the elements to exceed the particle size. Large amounts of Fe and Ni were revealed by the EDS analysis of P3 and P4.

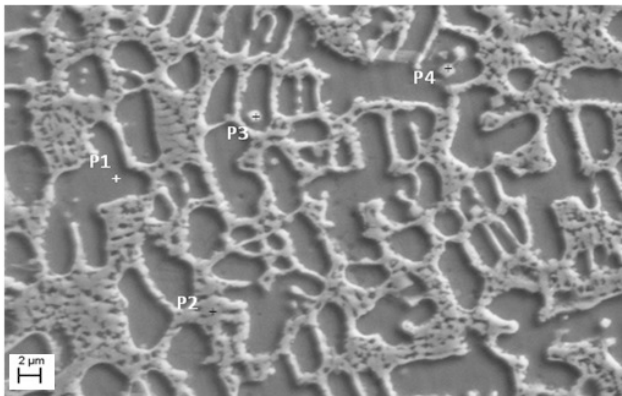


Fig. 8. Microstructure of the Ni60A+24%(SiC+Ti) composite coating

Table 3. EDS component analysis results for the Ni60A+24%(SiC+Ti) composite coating (mass fraction/%)

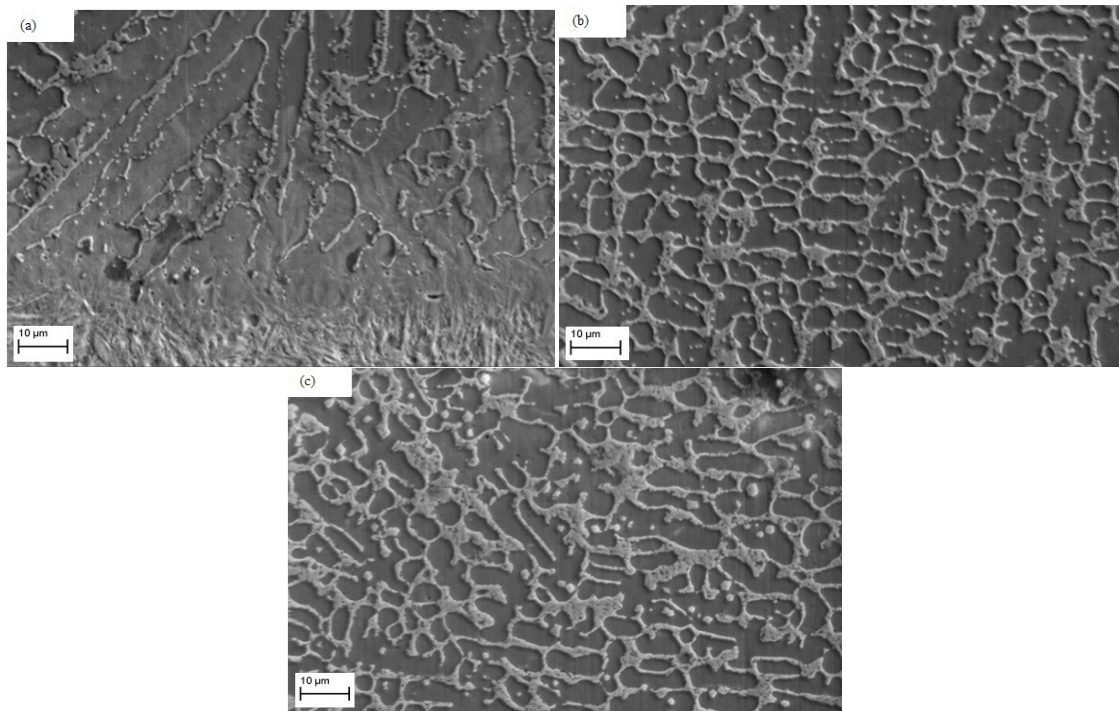
Position	Ni	Fe	Cr	Si	C	Ti	Total
dendritic structure (P1)	12.0	64.22	6.23	6.03	11.48	---	100
eutectic structure (P2)	9.34	61.21	6.61	3.18	19.20	0.10	100
particles (P3)	7.13	33.51	3.44	4.28	39.77	11.87	100
particles (P4)	6.08	28.88	4.92	4.38	41.94	13.80	100

4.3.3 Morphology and distribution of TiC

The mechanical property of the cladding layer depends on the morphology and distribution of TiC. The microstructures of the cladding layer at the top, middle, and bottom parts are shown in Figs. 9(a)–9(c), respectively. A large number of white particles were dispersed and distributed homogeneously on the dendritic structure, and such dispersion was beneficial for improving the abrasion resistance. The particle size increased from the bottom to the top part. The heat dissipation of the bottom part was better than that of the middle and top parts, and the undercool degree of the bottom part was larger. The grain nucleation rate was higher than the grain growth rate, resulting in the formation of fine grains at the bottom part. Although the particle size at the top part was the largest, the dendritic microstructure of TiC did not appear, which was conducive to the improvement of the mechanical property.

4.3.4 Influence of the composition content on the microstructure

To investigate the effect of composition content on the microstructure, laser cladding using the composite power with different composition contents was conducted at the laser power of 1000 W and the scanning speed of 125 mm/min.

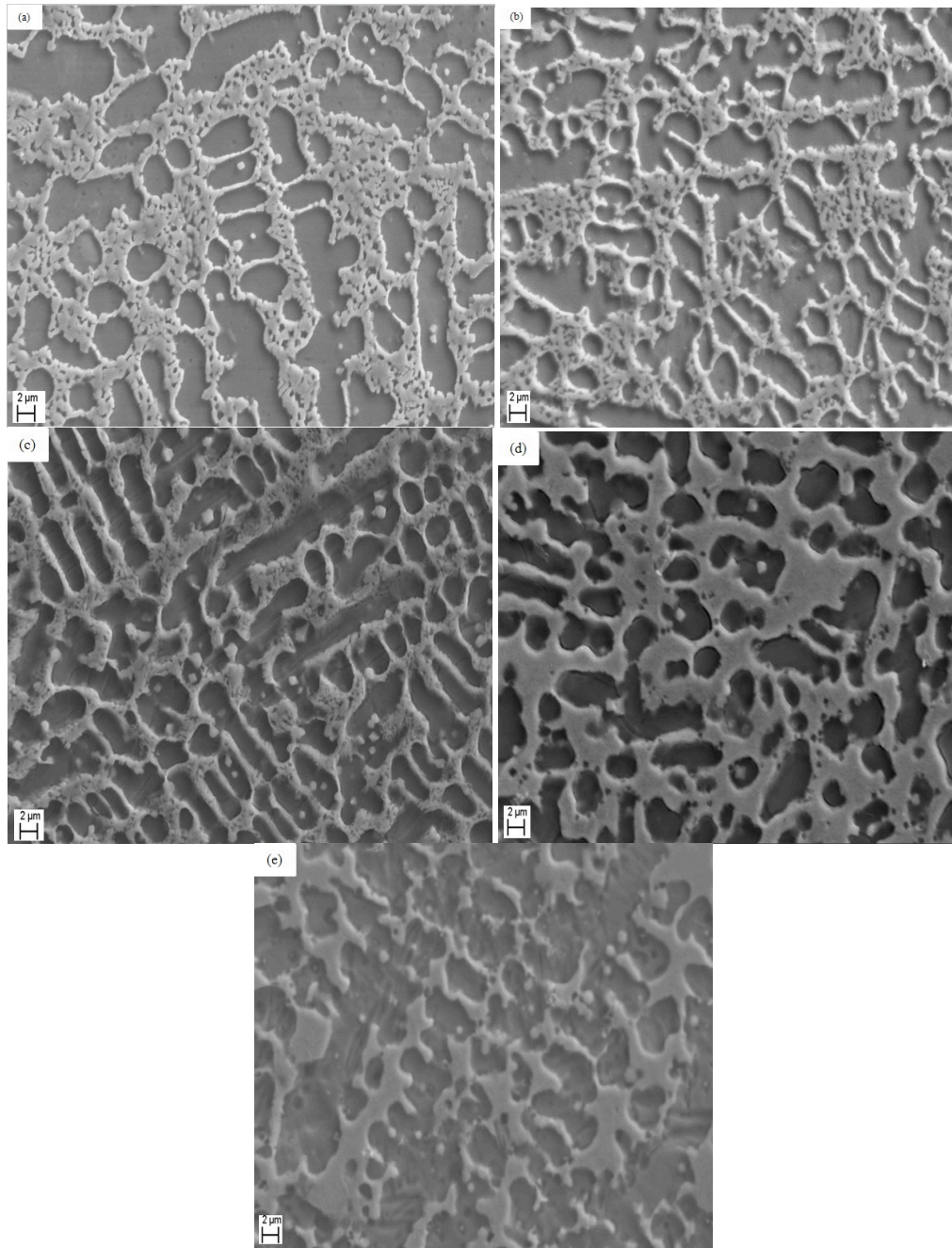


(a) The top of composite coating. (b) The middle of composite coating. (c) The bottom of composite coating
Fig. 9. Microstructure of different parts of the Ni60A+48%(SiC+Ti) composite coating

Fig. 10 shows the microstructure of the cladding layer with different composition contents. The middle part of the cladding layer was observed by SEM, which revealed that the microstructures of the cladding layer consisted of three phases, namely, the dendrites, the eutectic microstructure, and the TiC particles. The coarse dendrites gradually became smaller and disorderly as the (SiC+Ti) content was increased. In view of the content decline of the self-melting Ni60A alloy, the melting point of the composite powder increased as the (SiC+Ti) content increased. As the melting point increased at the same laser power, the absorbed energy was reduced, the melting degree of the powder decreased, and the undercool degree increased, resulting in a grain nucleation rate that is higher than the grain growth rate.

Thus, fine grains appeared. The distribution of dendrites became disordered due to the irregular direction of the heat dissipation.

A number of TiC particles existed. The number and size of particles were small, as shown in Fig.10(a). The number and size of TiC particles obviously increased as the (SiC+Ti) content increased, as depicted in Figs. 10(b)–10(e). The TiC content was positively correlated with the (SiC+Ti) content, demonstrating that the reaction that formed TiC was feasible under the given conditions. Otherwise, the TiC particles were dispersed and distributed homogeneously, and the size became less than 1 μm . These characteristics were beneficial for improving the hardness and the abrasion resistance.



(a) Ni60A+12%(SiC+Ti). (b) Ni60A+24%(SiC+Ti).

(c) Ni60A+36%(SiC+Ti). (d) Ni60A+48%(SiC+Ti). (e) Ni60A+60%(SiC+Ti)

Fig. 10. Microstructure of the cladding layers made of different materials

5. Conclusions

To study the reinforcement of Ni-based composite powder on a steel surface by laser cladding, the laser cladding parameters, microstructure, and phase composition were comprehensively analyzed. The notable conclusions of this work are as follows:

(1) The cladding composite coating with Ni60A+x%(SiC+Ti) composite powder as the raw material was produced on 45 steel surface by laser cladding. The main phases of the cladding composite coating were the γ -(Ni, Fe) solid solution, the intermetallic compound $Cr_{1.36}Fe_{0.52}$, the eutectic compounds $Ni_{16}Cr_6Si_7$, and the carbide TiC. The steel surface can be reinforced using the composite powder of Ni60A+x%(SiC+Ti) as the raw material to form in-situ TiC particles.

(2) Laser power significantly affected the macroscopic morphology and hardness of the cladding layer. The influence of the scanning speed was insignificant. When the (SiC+Ti) content was 24%, the optimal process parameters were the laser power of 800 W and the scanning speed of 125 mm/min.

(3) A large number of TiC particles were dispersed and distributed at the cladding layer. The morphology and the microstructure were influenced by the composition content

of SiC+Ti. The size and number of TiC gradually increases as the (SiC+Ti) content increased.

This study proposed the method of laser cladding of Ni-based Ni60A+x%(SiC+Ti) composite powder on 45 steel surface to form TiC particle reinforced coating and proved the feasibility of this method. The process parameters of laser power, scanning speed, and composition proportion were determined and optimized. The findings of this study provide guidance to practical application of laser cladding. However, in this study, only laser power, scanning speed, and composition proportion were studied. Thus, more process parameters should be considered in future studies to further improve the process level and material organization properties.

Acknowledgements

This work was supported by the Key Research Project of Henan Province Department of Education (Project No.18B460012), Science and Technology Research Project of Henan Province (Project No. 182102210468).

This is an Open Access article distributed under the terms of the Creative Commons Attribution License



References

1. Zhang M. X., Cao L., Wang Y. Y., Wang Y., "Corrosion-resistance and tribological properties of electroless Ni-B coatings on 45 steel". *China Surface Engineering*, 28(3), 2015, pp. 63-69.
2. Song J. L., Li Y. T., Deng Q. L., Hu D. J., "Research Progress of Laser Cladding Forming Technology". *Journal of Mechanical Engineering*, 46(14), 2010, pp.29-39.
3. Liu J. L., Yu H. J., Chen C. Z., Weng F., Dai J. J., "Research and development status of laser cladding on magnesium alloys: A review". *Optics and Lasers in Engineering*, 93, 2017, pp. 195-210.
4. Sui Y. Y., Yang F., Qin G. L., Ao Z. Y., Liu Y., Wang Y. B., "Microstructure and wear resistance of laser-cladded Ni-based composite coatings on downhole tools". *Journal of Materials Processing Tec*, 252, 2018, pp. 217-224.
5. Yan H., Zhang P.L., Gao Q.S., Qin Y., Li R. D., "Laser cladding Ni-based alloy/nano-Ni encapsulated h-BN self-lubricating composite coatings". *Surface & Coatings Technology*, 332, 2017, pp. 422-427.
6. Li Y. L., Bai X. B., Wang L., Ma M. L., Xi S. M., "Microstructure and wear-resistance property of laser cladding Ni-based alloy". *Ordnance Material Science and Engineering*, 33(6), 2010, pp. 26-29.
7. Song L. J., Zeng G.C., Xiao H., Xiao X. F., Li S. M., "Repair of 304 stainless steel by laser cladding with 316L stainless steel powders followed by laser surface alloying with WC powders". *Journal of Manufacturing Processes*, 24, 2016, pp.116-124.
8. Li J. N., Chen C. Z., He Q. S., "Influence of Cu on microstructure and wear resistance of TiC/TiB/TiN reinforced Composite coating fabricated by laser cladding". *Materials Chemistry and Physics*, 133, 2012, 741-745.
9. Chen J. M., Wang L. Q., Zhou J. S., Deng Z. C., Bao M., "Research progress of laser clad Ni-based Coatings". *China Surface Engineering*, 24(2), 2011, pp. 13-21.
10. Cao Y. B., Ren H. T., Hu C. SH., Meng Q. X., Liu Q., "In-situ formation behavior of NbC-reinforced Fe-based laser cladding coatings". *Materials Letters*, 147, 2015, pp. 61-63.
11. Liu H.G., Zhang X. W., Jiang Y. H., Zhou R., "Microstructure and high temperature oxidation resistance of in-situ synthesized TiN/Ti₃Al intermetallic composite coatings on Ti6Al4V alloy by laser cladding process". *Journal of Alloys and Compound*, 670, 2016, pp. 268-274.
12. Lu W. J., Guo X. L., Wang L. Q., Wang L. Q., Qin J. N., Zhang D., "Progress on in-situ discontinuously reinforced titanium matrix composites". *Journal of Aeronautical Materials*, 34(4), 2014, pp. 139-146.
13. Wang F., Chen C. ZH., Yu H. J., "Research status of laser cladding on titanium and its alloys: a review". *Materials & Design*, 58, 2014, pp. 412-425.
14. Liu K., Li Y. J., Wang J., Ma Q., "Effect of high dilution on the in-situ synthesis of Ni-Zr/Zr-Si(B, C) reinforced composite coating on zirconium alloy substrate by laser cladding". *Materials & Design*, 87, 2015, pp. 66-74.
15. Li Q. T., Lei Y. P., Fu H.G., "Growth Characteristics and Reinforcing Behavior of In-situ NbCp in Laser Cladded Fe-based Composite Coating". *Journal of Materials Science & Technology*, 31, 2015, pp. 766-772.
16. Zhang H., Chong K., Zhao W., Sun Z. P., "Laser cladding in-situ micro and sub-micro/nano Ti-V carbides reinforced Fe-based layers by optimizing initial alloy powders size". *Materials Letters*, 220, 2018, pp. 44-46.
17. Yu H.L., Zhang W., Wang H.M., Ji X.C., Song Z.Y., Li X.Y., Xu B.S., "In-situ synthesis of TiC/Ti composite coating by high frequency induction cladding". *Journal of Alloys and Compounds*, 701, 2017, pp. 244-255.
18. Zhou SH. F., Lei J. B., Dai X. Q., Guo J. B., Gu ZH. J., Pan H. B., "A comparative study of the structure and wear resistance of NiCrBSi/50 wt.% WC composite coatings by laser cladding and laser induction hybrid cladding". *Int. Journal of Refractory Metals and Hard Materials*, 60, 2016, pp. 17-27.
19. Andre C., Getúlio D. V., Danilo M. B., Raonei A. C., Vladimir J. T., Evaldo J. C., "Laser cladding of SiC multilayers for diamond deposition on steel substrates". *Diamond & Related Materials*, 65, 2016, pp. 105-114.
20. Zhang X. H., Chao M. J., Liang E. J., Yuan B., "In-situ synthesis of TiC-ZrC particulate reinforced Ni-based composite coatings by laser cladding". *Chinese Journal of Lasers*, 36(4), 2009, pp. 998-1006.
21. Du B. S., Zou Z. D., Wang X. H., Qu S., "In-situ synthesis of TiB₂/Fe composite coating by laser cladding". *Materials Letters*, 62(4-5), 2008, pp. 689-691.
22. Gao Y. L., Wang C. S., Yao M., Liu H., "The resistance to wear and corrosion of laser-cladding Al₂O₃ ceramic coating on Mg alloy". *Applied Surface Science*, 253(12), 2007, 5306-5311.
23. Lo K.H., Cheng F.T., Kwok C.T., Man H.C., "Improvement of cavitation erosion resistance of AISI 316 stainless steel by laser surface alloying using fine WC powder". *Surface and Coatings Technology*, 165, 2003, pp. 258-267.

24. Subrata K. G., Partha S., "Crack and wear behavior of SiC particulate reinforced aluminium based metal matrix composite fabricated by direct metal laser sintering process". *Materials and Design*, 32, 2011, pp. 139-145.
25. Bandar A., Dariusz G., Yang J. M., "In-situ formation of novel TiC-particle-reinforced 316L stainless steel bulk-form composites by selective laser melting". *Journal of Alloys and Compounds*, 706, 2017, pp. 409-418.
26. Zhang L., Wang C. SH., Han L. Y., Dong CH., "Influence of laser power on microstructure and properties of laser clad Co-based amorphous composite coatings". *Surfaces and Interfaces*, 6, 2017, pp.18-23.
27. Ali E., Stephen F., Corbin, Amir K., "The influence of combined laser parameters on in-situ formed TiC morphology during laser cladding". *Surface & Coatings Technology*, 206, 2011, pp.124-131.
28. Chinmaya K. S., Manoj M., "Effect of pulse laser parameters on TiC reinforced AISI 304 stainless steel composite coating by laser surface engineering process". *Optics and Lasers in Engineering*, 67, 2015, pp. 36-48.
29. Zeng CH., Tian W., Liao W. H., Liang H. "Microstructure and porosity evaluation in laser-cladding deposited Ni-based coatings". *Surface & Coatings Technology*, 294, 2016, pp.122-130.
30. Guo Y. Q., Sun R. L., Lei Y. W., Guo X.H. "Microstructure and properties of in-situ formed TiC particle reinforced Ni-base composite coating by laser cladding". *Transactions of Materials and Heat Treatment*, 30(3), 2009, pp.178-182,191.
31. Li S.N., H.P. Xiong , Li N., Chen B.Q., Gao C., Zou W.J., Ren H.S., "Mechanical properties and formation mechanism of Ti/SiC system gradient materials fabricated by in-situ reaction laser cladding". *Ceramics International*, 43, 2017, pp. 961-967.